

PERFORMANCE OF THERMAL BARRIER COATINGS IN HIGH HEAT FLUX ENVIRONMENTS*

ROBERT A. MILLER AND CHRISTOPHER C. BERNDT

Lewis Research Center, National Aeronautics and Space Administration, Cleveland, OH 44135 (U.S.A.)

(Received March 19, 1984; accepted April 9, 1984)

Thermal barrier coatings were exposed to the high temperature and high heat flux produced by a 30 kW plasma torch. Analysis of the specimen heating rates indicates that the temperature drop across the thickness of the 0.038 cm ceramic layer was about 1100°C after 0.5 s in the flame. An as-sprayed $\text{ZrO}_2\text{-8wt.}\% \text{Y}_2\text{O}_3$ specimen survived 3000 of the 0.5 s cycles without failing. Surface spalling was observed when 2.5 s cycles were employed but this was attributed to uneven heating caused by surface roughness. This surface spalling was prevented by smoothing the surface with silicon carbide paper or by laser glazing. A coated specimen with no surface modification but which was heat treated in argon also did not surface spall. Heat treatment in air led to spalling in as early as one cycle from heating stresses. Failures at edges were investigated and shown to be a minor source of concern. Ceramic coatings formed from $\text{ZrO}_2\text{-12wt.}\% \text{Y}_2\text{O}_3$ or $\text{ZrO}_2\text{-20wt.}\% \text{Y}_2\text{O}_3$ were shown to be unsuited for use under the high heat flux conditions of this study.

1. INTRODUCTION

A thermal barrier coating system with sufficient durability to survive on airfoil surfaces in a research gas turbine engine with moderately high heat fluxes and moderately high temperatures was first reported in the mid-1970s^{1,2}. However, this early thermal barrier coating system, which consisted of a layer of air-plasma-sprayed $\text{ZrO}_2\text{-12wt.}\% \text{Y}_2\text{O}_3$ applied directly over a layer of air-plasma-sprayed Ni-Cr-Al-Y bond coat, was unable to survive in an advanced research gas turbine engine³. Thermal barrier coatings have now been improved to the extent that they are used in revenue service on vane platforms in advanced commercial gas turbine engines⁴. Among the more significant advances responsible for this current success is the discovery that a $\text{ZrO}_2\text{-8wt.}\% \text{Y}_2\text{O}_3$ coating is much more durable than the earlier $\text{ZrO}_2\text{-12wt.}\% \text{Y}_2\text{O}_3$ version⁵. Possible reasons for this have been discussed by Miller et al.⁶

In the future, advanced engines operating at heat fluxes greater than those

* Paper presented at the International Conference on Metallurgical Coatings, San Diego, CA, U.S.A., April 9–13, 1984.

characteristic of current engines will require thermal barrier coatings for protecting airfoil surfaces. The testing which has led to advances in coating performance has been conducted in the low to moderate heat flux environment of furnaces and burner rigs. The initiation of coating failure in such rigs is associated with thermal expansion mismatch strain encountered on cooling and with time-at-temperature effects such as bond coat oxidation and plastic deformation⁷. Strains encountered on heating in such rigs are not severe enough to initiate coating failure⁷. It is not yet known whether strains encountered on heating in a gas turbine engine are severe enough to contribute to failure initiation.

Therefore testing procedures must be devised that allow determination of when the thermal loads developed on rapid heating become severe enough to initiate coating failure. This information may then be used to guide the processing of coatings for improved tolerance to such loads. In this study, a commercial plasma torch has been used as a high heat flux source. Various plasma-sprayed $ZrO_2-Y_2O_3$ thermal barrier coating systems were exposed in this rig and the response of these coatings to the high heat flux environment generated was characterized.

The plasma torch rig used for this study is intended to serve as an interim rig until a high pressure burner rig and a rocket engine test rig dedicated to materials research are available at the Lewis Research Center. Precedents for this type of test exist^{8,9}. The torch is relatively simple and inexpensive to operate. Possible disadvantages of this rig include the small flame diameter and the extremely high gas temperature attained.

2. EXPERIMENTAL DETAILS

A schematic diagram of the test rig is shown in Fig. 1. The plasma torch shown is operated at a power level of 30 kW. The nitrogen arc gas flow rate was 2800 l h^{-1} . The distance from the exit nozzle of the torch to the specimen is 4.4 cm. Specimens are held in the flame for cycles of length 0.5, 2.5 or 5.0 s followed by 30, 75 or 120 s of forced air cooling. An additional 0.50 s is required for the specimen to move between the cooling position and the heating position, and specimen heating begins before the specimens are fully in the heating position. Therefore effective heating times may be taken as 0.1 s longer than the nominal times.

Test specimens were solid superalloy rods 1.3 cm in diameter. Usually the alloy

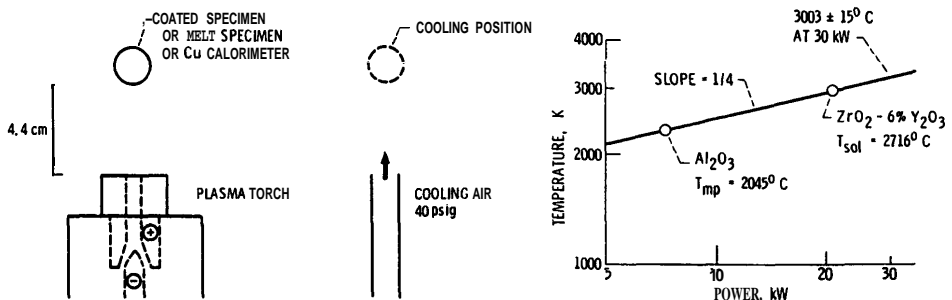


Fig. 1. Schematic diagram of a plasma torch test rig.

Fig. 2. Plasma torch arc power vs. apparent gas temperature.

was René 41. The thermal barrier coatings consisted of 0.013 cm of bond coat which was usually Ni-14wt.%Cr-14wt.%Al-0.1wt.%Zr under a 0.038 cm layer of plasma-sprayed $\text{ZrO}_2\text{-Y}_2\text{O}_3$ ceramic. The Y_2O_3 level was usually 8 wt.%; 12 and 20 wt.% Y_2O_3 ceramics were also investigated. Sintered starting powders were used for the 8 and 12 wt.% Y_2O_3 compositions while a non-reacted composite powder was used for the 20 wt.% Y_2O_3 composition.

Specimens were tested in the as-sprayed condition, after heat treating in air or in argon, and after surface treatment by smoothing with silicon carbide paper or laser glazing. The laser-glazed specimens were only available as hollow cylindrical specimens.

3. RESULTS AND DISCUSSION

3.1. Characterization of the plasma flame and of specimen heating rates

The apparent gas temperature of a 30 kW nitrogen plasma at a distance of 4.4 cm from the nozzle was determined through measurement of the power required to melt small samples of Al_2O_3 or $\text{ZrO}_2\text{-6wt.}\% \text{Y}_2\text{O}_3$. A plot of the logarithm of the known melting (or solidus) points *versus* the logarithm of the power required to melt the samples gives a line of slope 0.25 as shown in Fig. 2. This slope arises from the Stefan-Boltzmann relationship and is consistent with the assumption that heat is transferred from the cathode of the plasma torch to the plasma by radiation¹⁰ and from the gas to the samples by convection and conduction¹¹.

Extrapolation of the line in Fig. 2 to 30 kW yields an apparent flame temperature of 3000 °C. The actual gas temperature may differ somewhat since heat will be lost from the sample by radiation or gained by aerodynamic heating.

The coefficient of heat transfer from the gas to the sample was measured to be $0.2 \text{ W cm}^{-2} \text{ }^\circ\text{C}^{-1}$. A button calorimeter similar to those described in refs. 9 and 12 but of simplified design was used for this determination. The heat transfer coefficient and the apparent gas temperature were used to calculate the temperature distributions in the coated specimens as a function of time. A one-dimensional finite difference model was used for this calculation. The computer code employed was taken from ref. 13 (the reader is cautioned that there are several errors in the FORTRAN listing given in ref. 13). Values for the thermal conductivities and heat capacities of the bond coat and ceramic were taken from ref. 14. Values pertaining to 500 °C were used.

The calculated heating rates at the ceramic surface and at the interface with the bond coat are presented in Fig. 3. An initial response at 0.1 s was assumed as explained in the experimental section. Temperatures measured with a thermocouple centered 0.076 cm below the interface are also shown on the plot. These temperatures appear to be consistent with the calculated interface temperatures. The time at which the surface of the specimen was observed to be fully glowing in a 1/8000 s photograph is also indicated on the plot. This time corresponds to a calculated surface temperature of about 1100 °C, and the observation of glowing at this temperature seems plausible in view of the very short exposure time.

A very large AT between the surface and the interface has been achieved in this test. At 0.5 s this difference is almost 1100 °C. As shown in the figure this is much greater than the AT calculated for a 0.018 cm ceramic coating in a research gas

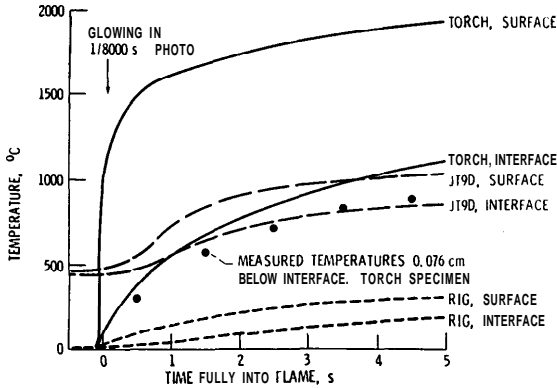


Fig. 3. Calculated heating rates at the ceramic layer surface and the interface with the bond coat for a 0.038 cm ceramic coating in the plasma torch (—) or Mach 0.3 burner rig (· · ·) or a 0.018 cm ceramic coating in a research gas turbine engine (---).

turbine engine during the **take-off** portion of the cycle³ and is greater still than the AT for a 0.038 cm coating in a Mach 0.3 burner rig¹⁵.

One can calculate the compressive thermal strain at the surface of the ceramic relative to the mean thermal strain in the ceramic from the expression¹⁶

$$\varepsilon = \alpha(\bar{T} - T_{\text{surf}}) \quad (1)$$

where α is the thermal expansion coefficient of the ceramic—about 10^{-5} (ref. 17)—and \bar{T} is the mean temperature in the ceramic layer. The values of the relative strain calculated from eqn. (1) are -0.57% , -0.48% and -0.42% at 0.5 s, 2.5 s and 5.0 s respectively. It may be noted that surface compressive strains are larger after 0.5 s than after 2.5 or 5.0 s. A complete calculation of strain would include ceramic-metal thermal expansion mismatch strains and residual stress.

From the above analysis it is apparent that the thermal loads imposed on coated specimens in this plasma torch rig are much more severe than those to be expected in a gas turbine engine.

3.2. Response of thermal barrier coating to high heat flux

The results of this investigation are displayed in Fig. 4. In this figure the composition of the ceramic, the pretreatment given to the specimen, the duration of the heat cycle and the type of failure observed (if any) are given. The total number of cycles is represented by the length of the bar. A pointed arrow indicates no failure. The test was terminated if no failure was observed after 1000 cycles of 0.5 s or after 100 cycles of 2.5 s. An exception was case A which ran for 3000 cycles before removal from the test.

Case A pertains to as-sprayed $\text{ZrO}_2\text{-8wt.}\% \text{Y}_2\text{O}_3$ ceramic and the lack of failure after 3000 cycles is quite encouraging. When the cycle duration was increased to 2.5 s or 5.0 s (cases B and C respectively) then surface spalling was observed after 15 cycles. This surface spalling was observed even though the relative surface strains at the end of the 0.5 s cycles exceeded those at the end of the 2.5 s cycles. A photograph of the surface of the specimen from case B is shown in Fig. 5. In case C the surface spalling was accompanied by surface melting even though the calculated

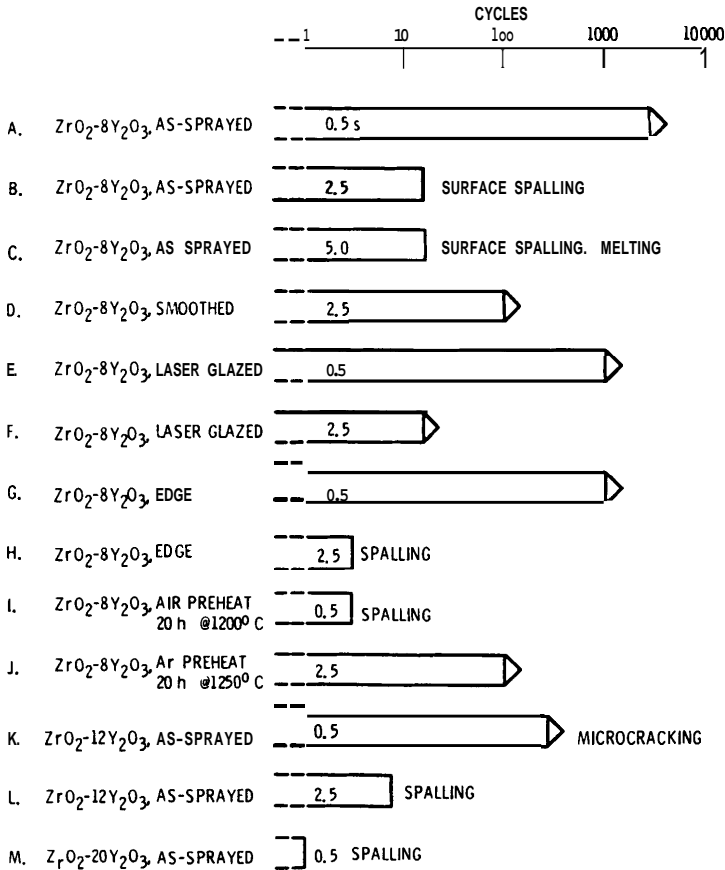


Fig. 4. Response of 0.038 cm ZrO₂-Y₂O₃ coatings to 0.5, 2.5 and 5.0s exposure cycles in a 30kW (3000°C) plasma flame.

temperature after 5 s (see Fig. 3) was about 800°C lower than the melting point of the ceramic. This indicates that there must be local hot spots on the rough surface. High speed photography indicated that some regions of the rough specimen began to glow almost 0.1 s before the surface came to a full glow. This local glowing occurs even before the specimen comes fully into position. Therefore it can be expected that there will be areas of severe local stress concentration at the rough surface of a specimen exposed to these very high temperatures.

Smoothing the coating surface with silicon carbide paper (case D and Fig. 6) prevents surface spalling. This smoothing reduced the measured roughness (arithmetic average) from about 10 μm to about 4 μm. A laser-glazed specimen did not surface spall after 15 2.5 s cycles (case F). The results for the laser-glazed specimen must be considered preliminary because the only specimens available at the time of this study were on hollow substrates which had previously been tested to failure in the hot zone region in a burner rig test. Regions away from the failure area were exposed in the plasma torch rig. The specimen in case F actually spalled after 20 cycles. However, at the present time it is not known whether this may have been due



Fig. 5. As-sprayed $\text{ZrO}_2\text{-8wt.\%Y}_2\text{O}_3$ specimen after 15 cycles of 2.5 s (case B) in a 30 kW plasma flame.

Fig. 6. Smoothed $\text{ZrO}_2\text{-8wt.\%Y}_2\text{O}_3$ specimen after 100 cycles of 2.5 s (case D) in a 30 kW plasma flame.



Fig. 7. Laser-glazed $\text{ZrO}_2\text{-8wt.\%Y}_2\text{O}_3$ specimen after the first 25 of a total of 1000 cycles of 0.5 s (case E) in a 30 kW plasma flame. The hot zone is near the bottom. Edge effect cracking of the coating occurs on the hollow specimen in the unglazed region near the top.

Fig. 8. Edge of a $\text{ZrO}_2\text{-8wt.\%Y}_2\text{O}_3$ specimen after three cycles (case H) in a 30 kW plasma flame.

to some factor such as overheating of the hollow specimen. The laser-glazed specimen in case E survived 1000 cycles of 0.5 s but it cracked and eventually spalled in the unglazed region near the upper edge as shown in Fig. 7. It should be noted that the cracks emanating from the unglazed areas dissipate once they reach the mudcracked laser-glazed region. Thus, even though the results on laser-glazed specimens are preliminary, this process (which has been discussed by Zaplatynsky¹⁸) is promising for high heat flux applications.

Since spalling had been observed at the edge of the hollow specimen in case E, the response of a solid specimen to heating at an edge was investigated. No edge effect spalling was observed after 1000 cycles of 0.5 s (case G). However, a minor amount of edge spalling was observed after three of the 2.5 s cycles (case H and Fig. 8).

Case I indicates that there is a strong correlation between oxidation and spalling on heating. A specimen which had received a relatively severe oxidative heat treatment—20 h at 1200°C in air—**spalled** in the first cycle in one test (Fig. 9) and in the third cycle in another test. Presumably the ceramic had been weakened near the interface with the bond coat as a result of strains induced by the formation of an oxide layer at the interface combined with thermal expansion mismatch strains encountered on cooling. A specimen heated for 20 h at 1250°C in an inert environment (case J and Fig. 10) did not **spall** and did not even surface **spall** after 100 cycles of 2.5 s.

A specimen coated with $\text{ZrO}_2\text{-12wt.\%Y}_2\text{O}_3$ was severely microcracked after

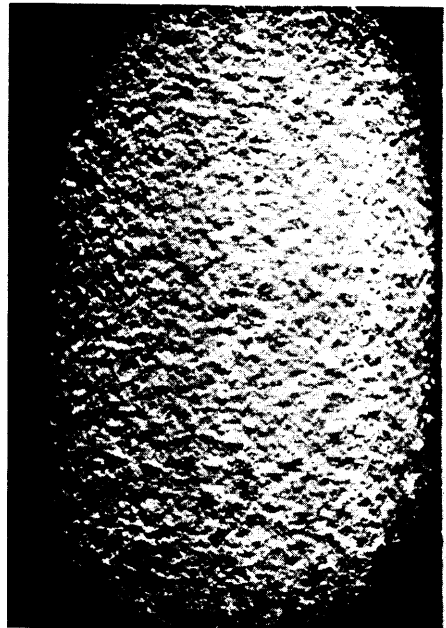


Fig. 9. Preoxidized $\text{ZrO}_2\text{-8wt.\%Y}_2\text{O}_3$ specimen (20 h at 1200°C main) after one 0.5 s cycle (case I) in a 30 kW plasma flame.

Fig. 10. $\text{ZrO}_2\text{-8wt.\%Y}_2\text{O}_3$ specimen (heat treated in argon for 20 h at 1250°C) after 100 cycles of 2.5 s (case J) in a 30 kW plasma.

250 cycles of 0.5 s (case K). This specimen was subsequently destroyed when it became stuck in the heating position. Another $\text{ZrO}_2\text{-12wt.}\% \text{Y}_2\text{O}_3$ specimen began to spall after seven 2.5 s cycles (case L). Three $\text{ZrO}_2\text{-20wt.}\% \text{Y}_2\text{O}_3$ specimens (case M) spalled during the first cycle.

4. CONCLUSION

The above results show that thermal barrier coatings with a ceramic layer based on $\text{ZrO}_2\text{-8wt.}\% \text{Y}_2\text{O}_3$ can withstand thermal strains greatly in excess of those expected in a gas turbine engine. Surface spalling associated with extremely high gas temperatures was encountered but this could be prevented by smoothing the surface with silicon carbide paper. Heat treatment in an inert environment may also prevent surface spalling. Results on laser-glazed specimens are preliminary, but it appears that glazed specimens also withstand heating stresses quite well.

Oxidation appears to induce spalling on heating. Thus oxidation has been implicated as a key factor in coating failure both in the heating mode in high heat flux plasma torch tests and in the cooling mode in moderate heat flux burner rig tests. This observation is cause for concern regarding the use of coatings for long periods of time in a high heat flux environment. Therefore the effects of oxidation require further investigation. Spalling at an edge may be a minor concern. Coatings formed from $\text{ZrO}_2\text{-12wt.}\% \text{Y}_2\text{O}_3$ or $\text{ZrO}_2\text{-20wt.}\% \text{Y}_2\text{O}_3$ were unsuitable for use at the high heat flux generated by the plasma torch.

REFERENCES

- 1 S. Stecura, NASA Tech. Memo. TM X-3425, 1976 (National Aeronautics and Space Administration).
- 2 C. H. Liebert, R. E. Jacobs, S. Stecura and C. R. Morse, NASA Tech. Memo. TM X-3410, 1976 (National Aeronautics and Space Administration).
- 3 W. R. Sevcik and B. L. Stoner, NASA Contract. Rep. CR-135360, 1978 (National Aeronautics and Space Administration; Pratt and Whitney Aircraft).
- 4 K. D. Sheffler, R. A. Graziani and G. C. Sinko, NASA Contract. Rep. **CR-167964**, 1982 (National Aeronautics and Space Administration; Pratt and Whitney Aircraft).
- 5 S. Stecura, NASA Tech. Memo. TM-78976, 1979 (National Aeronautics and Space Administration).
- 6 R. A. Miller, R. G. **Garlick** and J. L. Smialek, Am. Ceram. **Soc.**, Bull., 62 (1983) 1355.
- 7 R. A. Miller and C. E. Lowell, Thin Solid Films, 95 (1982) 265.
- 8 A. N. Curren, S. J. Grisaffe and K. C. Wycoff, NASA Tech. Memo. TM X-2461, 1972 (National Aeronautics and Space Administration).
- 9 H. E. Smith and J. C. Wurst, Rep. **ASD-TDR-623-655**, 1962 (Wright-Patterson Air Force Base).
- 10 C. W. Change and J. Szekely, **J. Met.**, 34 (1982) 57.
- 11 M. Usheo, J. Szekely and C. W. Chang, Ironmak. Steelmak., (1981) 279.
- 12 J. Hummik, Jr., High Temperature Inorganic Coatings, Reinhold, New York, 1963, pp. 197-198.
- 13 H. Schenk, Jr., **FORTRAN Methods** in Heat Flow, Ronald Press, New York, 1959, pp. 93-106.
- 14 P. A. Siemers and W. B. **Hillig**, NASA Contract. Rep. CR-165351, 1981 (National Aeronautics and Space Administration; General Electric Company).
- 15 G. McDonald and R. C. Hendricks, Thin Solid Films, 73 (1980) 491.
- 16 **S. S. Manson**, Thermal Stress and Low-Cycle Fatigue, **McGraw-Hill**, New York, 1966, p. 277.
- 17 C. C. Berndt and H. Herman, Ceram. Eng. Sci. Proc., 3 (1982) 792.
- 18 I. Zaplatynsky, Thin Solid Films, 95 (1982) 275.